

# Global Optimization by Basin-Hopping and the Lowest Energy Structures of Lennard-Jones Clusters Containing up to 110 Atoms

David J. Wales\*

University Chemical Laboratories, Lensfield Road, Cambridge CB2 1EW, U.K.

Jonathan P. K. Doye

FOM Institute for Atomic and Molecular Physics, Kruislaan 407, 1098 SJ Amsterdam, The Netherlands

Received: March 19, 1997; In Final Form: April 29, 1997<sup>⊗</sup>

We describe a global optimization technique using “basin-hopping” in which the potential energy surface is transformed into a collection of interpenetrating staircases. This method has been designed to exploit the features that recent work suggests must be present in an energy landscape for efficient relaxation to the global minimum. The transformation associates any point in configuration space with the local minimum obtained by a geometry optimization started from that point, effectively removing transition state regions from the problem. However, unlike other methods based upon hypersurface deformation, this transformation does not change the global minimum. The lowest known structures are located for all Lennard-Jones clusters up to 110 atoms, including a number that have never been found before in unbiased searches.

## I. Introduction

Global optimization is a subject of intense current interest.<sup>1</sup> Improved global optimization methods could be of great economic importance, since improved solutions to traveling salesman-type problems, the routing of circuitry in a chip, the active structure of a biomolecule, etc., equate to reduced costs or improved performance. In chemical physics the interest in efficient global optimization methods stems from the common problem of finding the lowest energy configuration of a (macro)molecular system. For example, it seems likely that the native structure of a protein is structurally related to the global minimum of its potential energy surface (PES). If this global minimum could be found reliably from the primary amino acid sequence, this knowledge would provide new insight into the nature of protein folding and save biochemists many hours in the laboratory. Unfortunately, this goal is far from being realized. Instead the development of global optimization methods has usually concentrated on much simpler systems.

Lennard-Jones (LJ) clusters represent one such test system. Here the potential is

$$E = 4\epsilon \sum_{i < j} \left[ \left( \frac{\sigma}{r_{ij}} \right)^{12} - \left( \frac{\sigma}{r_{ij}} \right)^6 \right]$$

where  $\epsilon$  and  $2^{1/6}\sigma$  are the pair equilibrium well depth and separation, respectively. We will employ reduced units, i.e.,  $\epsilon = \sigma = 1$  throughout. Much of the initial interest in LJ clusters was motivated by a desire to calculate nucleation rates for noble gases. However, as a result of the wealth of data generated, the LJ potential has been used not only for studying global optimization but also the effects of finite size on phase transitions such as melting. Through the combined efforts of many workers, likely candidates for the global minima of  $LJ_N$  clusters have been found up to  $N = 147$ .<sup>2–16</sup> This represents a significant achievement since extrapolation of Tsai and Jordan's comprehensive enumeration of minima for small LJ clusters<sup>17</sup> suggests that the PES of the 147-atom cluster possesses of the order of  $10^{60}$  minima.<sup>18</sup>

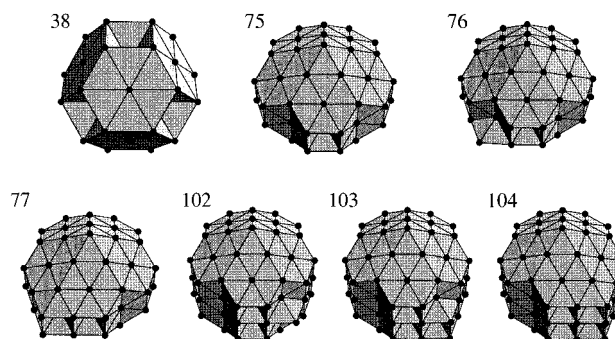


Figure 1. Nonicosahedral Lennard-Jones global minima.

Previous studies have revealed that the Mackay icosahedron<sup>19</sup> provides the dominant structural motif for LJ clusters in the size range of 10–150 atoms. Complete icosahedra are possible at  $N = 13, 55, 147, \dots$  At most intermediate sizes the global minimum consists of a Mackay icosahedron at the core covered by a low-energy overlayer. As a consequence of the phase behavior of LJ clusters, finding these global minima is relatively easy. Studies have shown that in the region of the solid–liquid transition the cluster is observed to change back and forth between a liquid-like form and icosahedral structures.<sup>20</sup> As a result of this “dynamic coexistence,” a method as crude as molecular dynamics within the melting region coupled with systematic minimization of configurations generated by the trajectory is often sufficient to locate the global minimum.<sup>21</sup>

However, there are a number of sizes at which the global minimum is not based on an icosahedral structure. These clusters are illustrated in Figure 1. For  $LJ_{38}$  the lowest energy structure is a face-centered-cubic (fcc) truncated octahedron,<sup>13,14</sup> and for  $N = 75, 76, 77, 102, 103,$  and  $104$ , geometries based on Marks' decahedra<sup>22</sup> are lowest in energy.<sup>14,15</sup> For these cases, finding the lowest minimum is much harder because the global minimum of free energy only becomes associated with the global potential energy minimum at temperatures well below melting where the dynamics of structural relaxation are very slow. For  $LJ_{38}$ , the microcanonical temperature for the transition from face-centered cubic to icosahedral structures has been estimated to be about  $0.12\epsilon k^{-1}$ , where  $k$  is the Boltzmann constant, and for

<sup>⊗</sup> Abstract published in *Advance ACS Abstracts*, June 15, 1997.

LJ<sub>75</sub> the estimate for the decahedral to icosahedral transition is about  $0.09\epsilon k^{-1}$ .<sup>23</sup> (For comparison, melting typically occurs at about  $T = 0.2-0.3\epsilon k^{-1}$ .)

The topography of the PES can also play a key role in determining the ease of global optimization.<sup>24</sup> A detailed study of the LJ<sub>38</sub> PES has shown that there is a large energy barrier between the fcc and icosahedral structures,<sup>25</sup> which correspond to well-separated regions of the PES. Furthermore, fcc and decahedral structures have less polytetrahedral character than icosahedral structures, and hence they have less in common with the liquid-like state, which is characterized by disordered polytetrahedral packing.<sup>26,27</sup> Since the vast majority of configuration space is dominated by “liquid-like” configurations, it is therefore harder to find global minima based upon fcc and decahedral packing using unbiased searches.

These considerations explain why global optimization methods have only recently begun to find the truncated octahedron<sup>13,16,28,29</sup> and why, until now, the Marks’ decahedron has never been found by an unbiased global optimization method. The greater difficulty of finding the LJ<sub>75</sub> global minimum compared to LJ<sub>38</sub> can probably be explained by the slightly smaller transition temperature, the sharper transition,<sup>23</sup> and the much larger number of minima on the LJ<sub>75</sub> PES.

Before we consider the effectiveness of different global optimization methods for Lennard-Jones clusters, it is interesting to note that the use of physical principles to construct good candidate structures for the global minima<sup>2-5,8,14,15</sup> or to reduce the configuration space that needs to be searched<sup>10-12</sup> led to the initial discovery of 93% of the LJ global minima in this size range. It seems that physical insight into a specific problem will often be able to beat unbiased global optimization, a view expressed by Ngo *et al.*<sup>30</sup> in their discussion of computational complexity.

One difficulty in evaluating the relative performances of different global optimization methods is that, too often, the methods have only been applied to small clusters, or to larger clusters with global minima that are especially stable, such as LJ<sub>55</sub>. It is also difficult to draw any firm conclusions about how efficient different methods may be when the number of searches employed varies widely. However, it seems reasonable to suggest two hurdles that any putative global optimization approach should aspire to. The first is the location of the truncated octahedron for LJ<sub>38</sub>, and any method which fails this test is unlikely to be useful. The second hurdle is the location of the Marks’ decahedron for LJ<sub>75</sub>; this problem poses a much more severe test for an unbiased search and one which does not appear to have been passed until the present work.

The most successful global optimization results for LJ clusters reported to date are for genetic algorithms.<sup>16,28,31,32</sup> These methods mimic some aspects of biological evolution: a population of clusters evolves to low energy by mutation and mating of structures, along with selection of those with low potential energy. To be successful, new configurations produced by “genetic manipulation” are mapped onto minima by a local optimization algorithm such as the conjugate gradient method. The study by Deaven *et al.* is particularly impressive, since these workers matched or beat all the lowest energy minima that they knew of up to  $N = 100$ , including the truncated octahedron (although they probably missed the global minima at  $N = 69$  and  $75-78$ ). Niese and Mayne were also able to locate the LJ<sub>38</sub> truncated octahedron, and report that this structure took about 25 times longer to find than the icosahedral global minima of the neighboring sizes.

Another class of global optimization techniques, sometimes called hypersurface deformation methods, attempts to simplify

the problem by applying a transformation to the PES which smoothes it and reduces the number of local minima.<sup>33,34</sup> The global minimum of the deformed PES is then mapped back to the original surface in the *hope* that this will lead back to the global minimum of the original PES. The distinctions between the various methods of this type lie in the type of transformations that are used, which include applying the diffusion equation,<sup>35</sup> increasing the range of the potential<sup>13,36</sup> and shifting the position of the potential minimum toward the origin.<sup>37</sup> The performance of hypersurface deformation methods has been variable: Pillardy and Piela<sup>13</sup> managed to find the 38-atom truncated octahedron, but other workers report difficulties<sup>35</sup> for the trivial cases of LJ<sub>8</sub> and LJ<sub>9</sub> where there are only 8 and 21 minima on the PES, respectively.

Although intuitively appealing, the problem with hypersurface deformation is that there is no guarantee that the global minimum on the deformed PES will map onto the global minimum of the original surface. This difficulty is clearly illustrated when we consider Stillinger and Stillinger’s suggestion of increasing the range of the potential:<sup>36</sup> it has been shown that the global minimum may in fact depend rather sensitively on the range of the potential, with the appearance of numerous “range-induced” transitions.<sup>14,38</sup>

Other methods include those based on “annealing”. Such approaches take advantage of the simplification in the free energy landscape that occurs at high temperatures and attempt to follow the free energy global minimum as the temperature is decreased. At 0 K, the free energy global minimum and the global minimum of the PES must coincide. Standard simulated annealing<sup>39</sup> was used by Wille to find a few new minima at small sizes<sup>9</sup> but does not appear to have been systematically applied to LJ clusters. More sophisticated variants of this technique include gaussian density annealing and analogues,<sup>40-43</sup> but again some appear to fail at small sizes.<sup>42,43</sup>

The difficulty with the annealing approach methods is that, if the free energy global minimum changes at low temperatures where dynamical relaxation is slow, the algorithms will become stuck in the structure corresponding to the high temperature free energy global minimum. Such methods are therefore likely to experience difficulties in finding the global minima for LJ<sub>38</sub> and LJ<sub>75</sub>. In the language employed in recent protein-folding literature,<sup>44</sup> annealing will fail when  $T_f < T_g$ , where  $T_f$  is the “folding” temperature below which the global potential energy and free energy minima coincide, and  $T_g$  is the “glass” temperature at which the system effectively becomes trapped in a local minimum.

Another method which attempts to reduce the effects of barriers on the PES makes use of quantum tunneling. The diffusion Monte Carlo approach is used to find the ground state wave function, which should become localized at the global minimum as  $\hbar$  is decreased to zero.<sup>45</sup> A more rigorous approach has been applied by Maranas and Floudas, who found upper and lower bounds for the energy of the global minimum. However, the computational expense of this method, which scales as  $2^N$  with the number of atoms, means that it has only been used for small systems.<sup>46,47</sup> Most of the above studies, along with the recently described “pivot method”<sup>48-50</sup> and “taboo search”,<sup>51,52</sup> have yet to prove their usefulness by passing the first hurdle for LJ<sub>38</sub> suggested above. However, this does not necessarily mean that these approaches should be discounted, since some authors have only applied their algorithms to smaller clusters and may not have run enough searches to achieve convergence.

In the present work we present the results of a “basin-hopping” global optimization technique for Lennard-Jones

TABLE 1: Global Minima of LJ<sub>N</sub> for N ≤ 110

N	point group	energy/ε	ref <sup>a</sup>	N	point group	energy/ε	ref <sup>a</sup>
2	D <sub>∞h</sub>	-1.000 000	2	57	C <sub>s</sub>	-288.342 625	10
3	D <sub>3h</sub>	-3.000 000	2/3	58	C <sub>3v</sub>	-294.378 148	10
4	T <sub>d</sub>	-6.000 000	2/3	59	C <sub>2v</sub>	-299.738 070	10
5	D <sub>3h</sub>	-9.103 852	2/3	60	C <sub>s</sub>	-305.875 476	10
6	O <sub>h</sub>	-12.712 062	2/3	61	C <sub>2v</sub>	-312.008 896	10
7	D <sub>5h</sub>	-16.505 384	2/3	62	C <sub>s</sub>	-317.353 901	10
8	C <sub>s</sub>	-19.821 489	2/3	63	C <sub>1</sub>	-323.489 734	10
9	C <sub>2v</sub>	-24.113 360	2/3	64	C <sub>s</sub>	-329.620 147	10
10	C <sub>3v</sub>	-28.422 532	2	65	C <sub>2</sub>	-334.971 532	12
11	C <sub>2v</sub>	-32.765 970	2	66	C <sub>1</sub>	-341.110 599	11/12
12	C <sub>5v</sub>	-37.967 600	2	67	C <sub>s</sub>	-347.252 007	10
13	I <sub>h</sub>	-44.326 801	2/3	68	C <sub>1</sub>	-353.394 542	10
14	C <sub>3v</sub>	-47.845 157	2/3	69	C <sub>5v</sub>	-359.882 566	present work
15	C <sub>2v</sub>	-52.322 627	2	70	C <sub>5v</sub>	-366.892 251	10
16	C <sub>s</sub>	-56.815 742	2	71	C <sub>5v</sub>	-373.349 661	10
17	C <sub>2</sub>	-61.317 995	7	72	C <sub>s</sub>	-378.637 253	11
18	C <sub>5v</sub>	-66.530 949	2	73	C <sub>s</sub>	-384.789 377	10
19	D <sub>5h</sub>	-72.659 782	2	74	C <sub>s</sub>	-390.908 500	10
20	C <sub>2v</sub>	-77.177 043	2	75	D <sub>5h</sub>	-397.492 331	14
21	C <sub>2v</sub>	-81.684 571	2	76	C <sub>s</sub>	-402.894 866	14
22	C <sub>s</sub>	-86.809 782	10	77	C <sub>2v</sub>	-409.083 517	14
23	D <sub>3h</sub>	-92.844 472	8	78	C <sub>s</sub>	-414.794 401	present work
24	C <sub>s</sub>	-97.348 815	9	79	C <sub>2v</sub>	-421.810 897	10
25	C <sub>s</sub>	-102.372 663	2	80	C <sub>s</sub>	-428.083 564	10
26	T <sub>d</sub>	-108.315 616	2	81	C <sub>2v</sub>	-434.343 643	10
27	C <sub>2v</sub>	-112.873 584	10	82	C <sub>1</sub>	-440.550 425	10
28	C <sub>s</sub>	-117.822 402	10	83	C <sub>2v</sub>	-446.924 094	10
29	D <sub>3h</sub>	-123.587 371	2	84	C <sub>1</sub>	-452.657 214	10
30	C <sub>2v</sub>	-128.286 571	10	85	C <sub>3v</sub>	-459.055 799	10
31	C <sub>s</sub>	-133.586 422	10	86	C <sub>1</sub>	-465.384 493	10
32	C <sub>2v</sub>	-139.635 524	10	87	C <sub>s</sub>	-472.098 165	10
33	C <sub>s</sub>	-144.842 719	10	88	C <sub>s</sub>	-479.032 630	16
34	C <sub>2v</sub>	-150.044 528	10	89	C <sub>3v</sub>	-486.053 911	10
35	C <sub>1</sub>	-155.756 643	10	90	C <sub>s</sub>	-492.433 908	10
36	C <sub>s</sub>	-161.825 363	10	91	C <sub>s</sub>	-498.811 060	10
37	C <sub>1</sub>	-167.033 672	10	92	C <sub>3v</sub>	-505.185 309	10
38	O <sub>h</sub>	-173.928 427	13/14	93	C <sub>1</sub>	-510.877 688	10
39	C <sub>5v</sub>	-180.033 185	10	94	C <sub>1</sub>	-517.264 131	10
40	C <sub>s</sub>	-185.249 839	10	95	C <sub>1</sub>	-523.640 211	10
41	C <sub>s</sub>	-190.536 277	10	96	C <sub>1</sub>	-529.879 146	10
42	C <sub>s</sub>	-196.277 534	10	97	C <sub>1</sub>	-536.681 383	10
43	C <sub>s</sub>	-202.364 664	10	98	C <sub>s</sub>	-543.642 957	16
44	C <sub>1</sub>	-207.688 728	10	99	C <sub>2v</sub>	-550.666 526	10
45	C <sub>1</sub>	-213.784 862	10	100	C <sub>s</sub>	-557.039 820	10
46	C <sub>2v</sub>	-220.680 330	10	101	C <sub>2v</sub>	-563.411 308	10
47	C <sub>1</sub>	-226.012 256	10	102	C <sub>2v</sub>	-569.363 652	15
48	C <sub>s</sub>	-232.199 529	10	103	C <sub>s</sub>	-575.766 131	15
49	C <sub>3v</sub>	-239.091 864	10	104	C <sub>2v</sub>	-582.086 642	15
50	C <sub>s</sub>	-244.549 926	10	105	C <sub>1</sub>	-588.266 501	10
51	C <sub>2v</sub>	-251.253 964	10	106	C <sub>1</sub>	-595.061 072	10
52	C <sub>3v</sub>	-258.229 991	10	107	C <sub>s</sub>	-602.007 110	present work
53	C <sub>2v</sub>	-265.203 016	10	108	C <sub>s</sub>	-609.033 011	10
54	C <sub>5v</sub>	-272.208 631	10	109	C <sub>1</sub>	-615.411 166	10
55	I <sub>h</sub>	-279.248 470	4	110	C <sub>s</sub>	-621.788 224	10
56	C <sub>3v</sub>	-283.643 105	10				

<sup>a</sup> The reference in which each minimum was first reported (to the best of our knowledge) is given. We intend to maintain an updated database of energies and coordinates for LJ and Morse clusters on our web site: <http://brian.ch.cam.ac.uk>.

clusters. All the known lowest energy structures up to  $N = 110$  have been located successfully, including three minima not previously reported. (See Tables 1 and 2.) This method is also the first unbiased algorithm to find the global minima based on the Marks decahedron around LJ<sub>75</sub> and LJ<sub>102</sub>. For reference, we collect the rather scattered results previously reported for LJ clusters to provide a complete catalog of the energies and point groups of the lowest energy minima that we know of. The results have been collected in the first entry of the Cambridge Cluster Database at <http://brian.ch.cam.ac.uk>.

## II. Method

The present approach has been guided by previous work on energy landscapes which has identified features that enable the

system to locate its global minimum efficiently.<sup>44</sup> In particular, analysis of model energy landscapes, using a master equation approach for the dynamics, has provided good evidence that such a surface should have a large potential energy gradient and the lowest possible transition state energies or rearrangement barriers.<sup>53</sup> These results immediately suggest a simple way to transform the PES which does not change the global minimum, nor the relative energies of any local minima. We consider the transformed energy  $\tilde{E}$  defined by

$$\tilde{E}(\mathbf{X}) = \min\{E(\mathbf{X})\}$$

where  $\mathbf{X}$  represents the  $3N$ -dimensional vector of nuclear coordinates and min signifies that an energy minimization is performed starting from  $\mathbf{X}$ . In the present work, energy

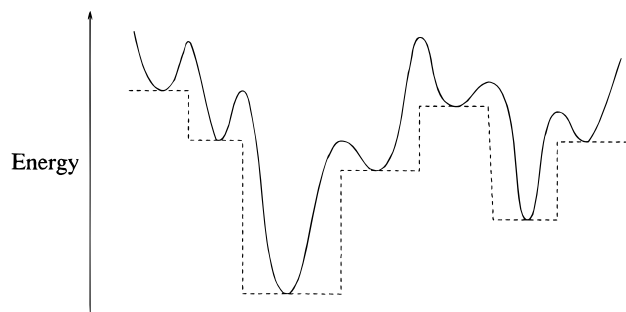


**Figure 2.** A schematic diagram illustrating the effects of our energy transformation for a one-dimensional example. The solid line is the energy of the original surface and the dashed line is the transformed energy  $\tilde{E}$ .

minimizations were performed using the Polak–Ribiere variant of the conjugate gradient algorithm.<sup>54</sup> Hence the energy at any point in configuration space is assigned to that of the local minimum obtained by the given geometry optimization technique, and the PES is mapped onto a set of interpenetrating staircases with plateaus corresponding to the set of configurations which lead to a given minimum after optimization. A schematic view of the staircase topography that results from this transformation is given in Figure 2. These plateaus, or basins of attraction, have been visualized in previous work as a means to compare the efficiency of different transition state searching techniques.<sup>55,56</sup>

The energy landscape for the function  $\tilde{E}(\mathbf{X})$  was explored using a canonical Monte Carlo simulation at a *constant* reduced temperature of 0.8. At each step, all coordinates were displaced by a random number in the range  $[-1,1]$  times the step size, which was adjusted to give an acceptance ratio of 0.5. The nature of the transformed surface allowed relatively large step sizes of between 0.36–0.40. For each cluster in the range considered, seven separate runs were conducted. Five of these each consisted of 5000 Monte Carlo steps starting from different randomly generated configurations of atoms confined to a sphere of radius 5.5 reduced units. The subsequent geometry optimizations employed a container of radius one plus the value required to contain the same volume per atom as the fcc primitive cell. The container should have little effect on any of our results and is only required to prevent dissociation during the conjugate gradient optimizations.

The convergence criterion employed for the conjugate gradient optimizations used in the Monte Carlo moves need not be very tight. In the present work we required the root-mean-square (RMS) gradient to fall below 0.01 in reduced units and the energy to change by less than  $0.1 \epsilon$  between consecutive steps in the conjugate gradient search. Initially it appeared that a tolerance of 0.1 for the RMS gradient was satisfactory, but this was subsequently found to cause problems for clusters containing more than about 60 atoms. The lowest energy structures obtained during the canonical simulation were saved and reoptimized with tolerances of  $10^{-4}$  and  $10^{-9}$  for the RMS force and the energy difference, respectively. The final energies are accurate to about six decimal places.

Several other techniques were employed in these calculations, namely seeding, freezing and angular moves. Here we used the pair energy per atom,  $E(i)$ , defined as

$$E(i) = 4\epsilon \sum_{j \neq i} \left[ \left( \frac{\sigma}{r_{ij}} \right)^{12} - \left( \frac{\sigma}{r_{ij}} \right)^6 \right]$$

so that the total energy is

$$E = \frac{1}{2} \sum_i E(i)$$

If the highest pair energy rose above a fraction  $\alpha$  of the lowest pair energy then an angular move was employed for the atom in question with all other atoms fixed.  $\alpha$  was adjusted to give an acceptance ratio for angular moves of 0.5 and generally converged to between 0.40 and 0.44. Each angular displacement consisted of choosing random  $\theta$  and  $\phi$  spherical polar coordinates for the atom in question, taking the origin at the center of mass and replacing the radius with the maximum value in the cluster.

The two remaining runs for each size consisted of only 200 Monte Carlo steps starting from the global minima obtained for the clusters containing one more and one less atom. When starting from  $\text{LJ}_{N-1}$  the  $N - 1$  atoms were frozen for the first 100 steps, during which only angular moves were attempted for the remaining atom, starting from a random position outside the core. When starting from  $\text{LJ}_{N+1}$  the atom with the highest pair energy  $E(i)$  was removed and 200 unrestricted Monte Carlo moves were attempted from the resulting geometry.

The above basin-hopping algorithm shares a common philosophy with our previous approach in which steps were taken directly between minima using eigenvector-following to calculate pathways.<sup>25</sup> The latter method is similar to that described recently by Barkema and Mousseau<sup>57</sup> in their search for well-relaxed configurations in glasses. Although the computational expense of transition state searches probably makes this method uncompetitive for global optimization, our study illustrated the possible advantage of working in a space in which only the minima are present. The basin-hopping algorithm differs in that it is applied in configuration space to a transformed surface, rather than in a discrete space of minima, and steps are taken stochastically. The genetic algorithms described by Deaven *et al.*<sup>16</sup> and Niese and Mayne<sup>28</sup> used conjugate gradient minimization to refine the local minima which comprise the population of structures that are evolved in their procedure. Hence these authors are in effect studying the same transformed surface as described above, but explore it in a rather different manner. We suspect that the success of their methods is at least partly due to the implicit use of the transformed surface  $\tilde{E}$ .

The present approach is basically the same as the “Monte Carlo-minimization” algorithm of Li and Scheraga,<sup>58</sup> who applied it to search the conformational space of the pentapeptide [Met<sup>5</sup>]enkephalin. A similar method has recently been used by Baysal and Meirovitch<sup>59</sup> to search the conformational space of cyclic polypeptides.

### III. Results

The basin-hopping algorithm has successfully located all the lowest known minima up to  $\text{LJ}_{110}$ , including all the nonicosahedral structures illustrated in Figure 1 (sizes 38, 75, 76, 77, 102, 103, and 104) and three new geometries based upon icosahedra illustrated in Figure 3 (sizes 69, 78, and 107). We believe that this is the first time any of the six decahedral global minima have been located by an unbiased algorithm. The total number of searches was fixed in our calculations to provide a simple reference criterion. In fact, most of the global minima were found in more than one of the separate Monte Carlo runs. The global minima for the smallest clusters were located within a few steps in each of the seven runs. To give a better idea of how the algorithm performed we will provide some more details for the sizes with nonicosahedral or newly discovered icosahedral global minima.

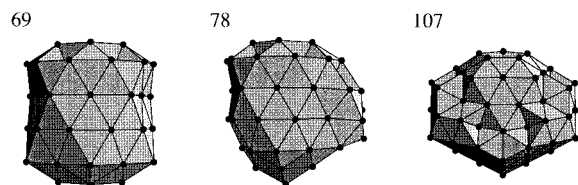


**Figure 3.** Lennard-Jones global minima that have not previously been reported.

**TABLE 2: Lowest Energy Icosahedral Minima at Sizes with Nonicosahedral Global Minima**

N	point group	energy/ $\epsilon$	ref
38	$C_{5v}$	-173.252 378	16
75	$C_1$	-396.282 249	14
76	$C_1$	-402.384 580	12
77	$C_1$	-408.518 265	12
102	$C_s$	-569.277 721	10
103	$C_1$	-575.658 879	10
104	$C_s$	-582.038 429	10

For LJ<sub>38</sub> the truncated octahedron was found in four out of five of the longer unseeded runs; the first success occurred within a thousand Monte Carlo steps on average. Not surprisingly, the global minimum was not located in the shorter runs starting from the structurally unrelated global minima for  $N = 37$  and 39.

For LJ<sub>75</sub> the global minimum was found in just one of the longer Monte Carlo runs, and again in the short run from the global minimum for LJ<sub>76</sub>. However, the latter minimum was only found in the short runs seeded from the LJ<sub>75</sub> and LJ<sub>77</sub> decahedra. Similarly, the LJ<sub>77</sub> global minimum was only found in the short run seeded from the LJ<sub>76</sub> decahedron. The decahedral global minimum for LJ<sub>75</sub> was found in four out of 100 Monte Carlo runs of 5000 steps each, a frequency which fits in quite well with our results for LJ<sub>75</sub>, LJ<sub>76</sub>, and LJ<sub>77</sub>. A successful run requires an initial geometry which falls within the decahedral catchment area; all the other runs produce the lowest icosahedral minimum after which the decahedron is not found. It would obviously be possible to locate global minima based upon decahedra more efficiently by biasing the starting configuration, but our intention was to analyze the performance of an unbiased algorithm in the present work.

The pattern for LJ<sub>75</sub>–LJ<sub>77</sub> is repeated for LJ<sub>102</sub>–LJ<sub>103</sub>. For LJ<sub>102</sub> the decahedral global minimum was located in one of the longer Monte Carlo runs and in the short run seeded from the global minimum of LJ<sub>103</sub>. The decahedral minima for LJ<sub>103</sub> and LJ<sub>104</sub> were only found in short runs seeded from larger or smaller decahedra. The decahedral global minimum for LJ<sub>102</sub> was found in three out of 100 Monte Carlo runs of 5000 steps each.

The three new icosahedral global minima all have an atom missing from a vertex of the underlying Mackay icosahedron (Figure 3). This is a possibility that Northby did not consider in his restricted search of the icosahedral configuration space. The new LJ<sub>69</sub> global minimum was found in three of the five longer Monte Carlo runs and in the short run seeded from LJ<sub>70</sub>. The new global minimum for LJ<sub>78</sub> was only found in the short run seeded from LJ<sub>79</sub>. The new minimum for LJ<sub>107</sub> was found in one of the longer Monte Carlo runs and in the short run seeded from LJ<sub>108</sub>.

We also performed a few preliminary runs for LJ<sub>192</sub> and LJ<sub>201</sub>, sizes at which a complete Marks decahedron and a complete truncated octahedron occur, respectively. For LJ<sub>192</sub> the Marks decahedron has energy -1175.697 144. This structure was not found in 50 MC runs of 10 000 steps each; instead the lowest minimum located had an energy of -1174.919 801. For LJ<sub>201</sub>

the truncated octahedron has energy -1232.731 497. However, we located a structure of energy -1236.124 253, which is based upon icosahedral packing. This minimum was found in three out of 50 MC runs of 10 000 steps each. For these larger systems greater efficiency could probably be achieved by varying the temperature and other parameters of the MC search.

#### IV. Conclusions

We have presented the results of a “basin-hopping” or “Monte Carlo-minimization”<sup>58</sup> approach to global optimization for atomic clusters bound by the Lennard-Jones potential containing up to 110 atoms. All the lowest known minima were located successfully, including the seven structures based upon fcc or decahedral packing and three new global minima based upon icosahedra. Of the latter ten structures, only the smallest has been located before by an unbiased algorithm, to the best of our knowledge.

The method is based upon a hypersurface deformation in which the potential energy surface (PES) is converted into the set of basins of attraction of all the local minima. This process removes all the transition state regions but does not affect the energies of the minima. On the original PES, most trajectories that approach the boundary between two basins of attraction are reflected back due to the high potential energy; only if the trajectory is along a transition state valley does passage between basins become likely. In contrast, on the transformed PES it is feasible for the system to hop between basins at any point along the basin boundary which dramatically reduces the time scale for interbasin motion. We speculate that the success of a previous genetic algorithm applied to the same clusters may be at least partly due to the fact that the same surface is implicitly considered in that approach.<sup>16</sup>

The efficiency of the present approach could doubtless be improved by combining it with various other techniques. The most obvious shortcut would be to start not from initial random configurations but from seeds with either decahedral, icosahedral, or fcc morphologies. We have already checked that such biasing is indeed effective, but our aim in the present paper was to gauge the performance of the unbiased algorithm. The temperature at which our Monte Carlo runs were conducted was also not optimized systematically.

Finally, as we noted in the introduction, global optimization for Lennard-Jones clusters at most sizes is a relatively easy task. A more stringent and general test is provided by Morse clusters which exhibit different structural behaviour as a function of the range of the potential.<sup>14,38</sup> At short range the task is particularly difficult because the PES is very rugged—the number of minima<sup>27</sup> and the barrier heights<sup>60</sup> increase as the range is decreased.

**Acknowledgment.** We are grateful to the Royal Society (D.J.W.) and the Engineering and Physical Sciences Research Council (J.P.K.D.) for financial support.

#### References and Notes

- (1) The magnitude of this interest can be gauged by, for example, the fact that there have been over 2600 citations of the classic simulated annealing paper by Kirkpatrick *et al.*, cited in ref 39.
- (2) Hoare, M. R.; Pal, P. *Adv. Phys.* **1971**, *20*, 161.
- (3) Hoare, M. R.; Pal, P. *Nature (Physical Sciences)* **1971**, *230*, 5.
- (4) Hoare, M. R.; Pal, P. *Nature (Physical Sciences)* **1972**, *236*, 35.
- (5) Hoare, M. R.; Pal, P. *Adv. Phys.* **1975**, *24*, 645.
- (6) Hoare, M. R. *Adv. Chem. Phys.* **1979**, *40*, 49.
- (7) Freeman, D. L.; Doll, J. D. *J. Chem. Phys.* **1985**, *82*, 462.
- (8) Farges, J.; de Feraudy, M. F.; Raoult, B.; Torchet, G. *Surf. Sci.* **1985**, *156*, 370.
- (9) Wille, L. T. *Chem. Phys. Lett.* **1987**, *133*, 405.
- (10) Northby, J. A. *J. Chem. Phys.* **1987**, *87*, 6166.

- (11) Coleman, T.; Shalloway, D. *J. Global Optimization* **1994**, *4*, 171.
- (12) Xue, G. L. *J. Global Optimization* **1994**, *4*, 425.
- (13) Pillardy, J.; Piela, L. *J. Phys. Chem.* **1995**, *99*, 11805.
- (14) Doye, J. P. K.; Wales, D. J.; Berry, R. S. *J. Chem. Phys.* **1995**, *103*, 4234.
- (15) Doye, J. P. K.; Wales, D. J. *Chem. Phys. Lett.* **1995**, *247*, 339.
- (16) Deaven, D. M.; Tit, N.; Morris, J. R.; Ho, K. M. *Chem. Phys. Lett.* **1996**, *256*, 195.
- (17) Tsai, C. J.; Jordan, K. D. *J. Phys. Chem.* **1993**, *97*, 11227.
- (18) The exact value of this figure should not be taken too seriously since it depends sensitively on the functional form used to fit Tsai and Jordan's results for the number of minima. The value given was obtained using the form  $\exp(a + bN)$ , but if one instead uses the form  $\exp(a + bN + cN^2)$  the estimate is of the order of  $10^{259}$  minima.
- (19) Mackay, A. L. *Acta Crystallogr.* **1962**, *15*, 916.
- (20) Kunz, R. E.; Berry, R. S. *Phys. Rev. Lett.* **1993**, *71*, 3987. Kunz, R. E.; Berry, R. S. *Phys. Rev. E* **1994**, *49*, 1895.
- (21) For the larger sizes coexistence in the melting region may occur between the liquid-like state and defective structures based on the global minimum,<sup>20</sup> and hence molecular dynamics runs at two energies would probably be necessary, first in the melting region and then at a lower energy starting from one of the defective icosahedral structures generated.
- (22) Marks, L. D. *Philos. Mag. A* **1984**, *49*, 81.
- (23) These temperatures were calculated using the harmonic superposition method (Wales, D. J. *Molec. Phys.* **1993**, *78*, 151) in the same manner as described in ref 14 for a 75-atom cluster bound by the Morse potential. Note that a  $\gamma(E')$ , incorrectly appears in the relevant equation in ref 14.
- (24) Doye, J. P. K.; Wales, D. J. *J. Chem. Phys.* **1996**, *105*, 8428.
- (25) Doye, J. P. K.; Wales, D. J. *Z. Phys. D* **1997**, in press.
- (26) Nelson, D. R.; Spaepen, F. *Solid State Phys.* **1989**, *42*, 1.
- (27) Doye, J. P. K.; Wales, D. J. *Science* **1996**, *271*, 484. Doye, J. P. K.; Wales, D. J. *J. Phys. B* **1996**, *29*, 4859.
- (28) Niesse, J. A.; Mayne, H. R. *J. Chem. Phys.* **1996**, *105*, 4700.
- (29) Barron, C.; Gomez, S.; Romero, D. *Appl. Math. Lett.* **1996**, *5*, 75.
- (30) Ngo, J. T.; Marks, J.; Karplus, N. In *The Protein Folding Problem and Tertiary Structure Prediction*; Merz, K., Le Grand, S., Eds.; Birkhäuser: Boston, 1994.
- (31) Gregurick, S. K.; Alexander, M. H.; Hartke, B. *J. Chem. Phys.* **1996**, *104*, 2684.
- (32) Mestres, J.; Scuseria, G. E. *J. Comput. Chem.* **1995**, *16*, 729.
- (33) Stillinger, F. H.; Weber, T. A. *J. Stat. Phys.* **1988**, *52*, 1429.
- (34) Piela, L.; Olszewski, K. A.; Pillardy, J. *J. Mol. Struct. (THEOCHEM)* **1994**, *308*, 229.
- (35) Kostrowicki, J.; Piela, L.; Cherayil, B. J.; Scheraga, H. A. *J. Phys. Chem.* **1991**, *95*, 4113. Scheraga, H. A. *Int. J. Quant. Chem.* **1992**, *42*, 1529.
- (36) Stillinger, F. H.; Stillinger, D. K. *J. Chem. Phys.* **1990**, *93*, 6106. Head-Gordon, T.; Stillinger, F. H.; Stillinger, D. K. *Proc. Natl. Acad. Sci. U.S.A.* **1991**, *88*, 11076.
- (37) Pillardy, J.; Olszewski, K. A.; Piela, L. *J. Phys. Chem.* **1992**, *96*, 4337.
- (38) Doye, J. P. K.; Wales, D. J. *J. Chem. Soc., Faraday Trans.* **1997**. Submitted for publication.
- (39) Kirkpatrick, S.; Gelatt, C. D.; Vecchi, M. P. *Science* **1983**, *220*, 671.
- (40) Ma, J.; Hsu, D.; Straub, J. E. *J. Chem. Phys.* **1993**, *99*, 4024.
- (41) Ma, J.; Straub, J. E. *J. Chem. Phys.* **1994**, *101*, 533.
- (42) Tsou, C.; Brooks, C. L. *J. Chem. Phys.* **1994**, *101*, 6405.
- (43) Schelstrate, S.; Verschelde, H. *J. Phys. Chem. A* **1997**, *101*, 310.
- (44) Bryngelson, J. D.; Onuchic, J. N.; Socci, N. D.; Wolynes, P. G. *Proteins* **1995**, *21*, 167.
- (45) Finnila, A. B.; Gomez, M. A.; Sebenink, C.; Stenson, C.; Doll, J. D. *Chem. Phys. Lett.* **1996**, *219*, 343.
- (46) Maranas, C. D.; Floudas, C. A. *J. Chem. Phys.* **1992**, *97*, 7667.
- (47) Maranas, C. D.; Floudas, C. A. *J. Chem. Phys.* **1994**, *100*, 1247.
- (48) Stanton, A. F.; Bleil, R. E.; Kais, S. *J. Comput. Chem.* **1997**, *18*, 594.
- (49) Serra, P.; Stanton, A. F.; Kais, S. *Phys. Rev. E* **1997**, *55*, 1162.
- (50) Serra, P.; Stanton, A. F.; Kais, S.; Bleil, R. E. *J. Chem. Phys.* **1997**, *106*, 7170.
- (51) Cvijovic, D.; Klinowski, J. *Science* **1995**, *267*, 664.
- (52) Hong, S. D.; Jhon, M. S. *Chem. Phys. Lett.* **1997**, *267*, 422.
- (53) Doye, J. P. K.; Wales, D. J. *J. Chem. Phys.* **1996**, *105*, 8428.
- (54) Press, W. H.; Flannery, B. P.; Teukolsky, S. A.; Vetterling, W. T. *Numerical Recipes* Cambridge University Press: Cambridge, 1986.
- (55) Wales, D. J. *J. Chem. Soc., Faraday Trans.* **1992**, *88*, 653.
- (56) Wales, D. J. *J. Chem. Soc., Faraday Trans.* **1993**, *89*, 1305.
- (57) Barkema, G. T.; Mousseau, N. *Phys. Rev. Lett.* **1996**, *77*, 4358.
- (58) Li, Z.; Scheraga, H. A. *Proc. Natl. Acad. Sci. U.S.A.* **1987**, *84*, 6611.
- (59) Baysal, C.; Meirovitch, H. *J. Chem. Phys.* **1996**, *105*, 7868.
- (60) Wales, D. J. *J. Chem. Phys.* **1994**, *101*, 3750.